Final version available at http://www.sciencedirect.com/science/article/pii/S0033589409001112

The last interglacial sea-level high stand on the southern Cape Coastline of South Africa

Andrew S. Carr [a], Mark D. Bateman [b], David L. Roberts [c], Colin V. Murray-Wallace [d] Zenobia Jacobs [d] and Peter J. Holmes [e].

[a] *Department of Geography, University of Leicester University Road, Leicester LE1 7RH*

[b]*Sheffield Centre for International Drylands Research, Department of Geography, University of Sheffield, Winter Street, Sheffield, S10 2TN, UK.*

[c]*Council for Geoscience, PO Box 572, Bellville 7535, South Africa*

[d] *GeoQuEST Research Centre, School of Earth and Environmental Sciences, University of Wollongong, NSW, 2522, Australia*

[e] *Department of Geography, University of the Free State, PO Box 339, Bloemfontein 9300, South Africa*

Final version available at http://www.sciencedirect.com/science/article/pii/S0033589409001112

Abstract

The continental margin of southern South Africa exhibits an array of emergent marginal marine sediments permitting the reconstruction of long-term eustatic sea-level changes. We report a suite of optical luminescence ages and supplementary amino acid racemization data, which provide paleosea-level index points for three sites on this coastline. Deposits in the Swartvlei and Groot Brak estuaries display tidal inlet facies overlain by shoreface or eolian facies. Contemporary facies relations suggest a probable high stand 6.0-8.5 m above modern sea level (amsl). At Cape Agulhas, evidence of a past sea-level high stand comprises a gravel beach (ca. 3.8 m amsl) and an overlying sandy shoreface facies (up to 7.5 m amsl). OSL ages between 138 ± 7 ka and 118 ± 7 ka confirm a last interglacial age for all marginal marine facies. The high stand was followed by a sea-level regression associated with the accumulation of eolian dunes dating to 122 ± 7 ka to 113 ± 6 ka. These data provide the first rigorous numerical age constraints for last interglacial sea-level fluctuations in this region, revealing the timing and elevation of the last interglacial high stand to broadly mirror a number of other far-field locations.

Final version available at http://www.sciencedirect.com/science/article/pii/S0033589409001112

Introduction

The importance of constraining the timing and amplitudes of past sea-level changes has long been recognized (Bard et al., 1990; Stirling et al., 1995; Lambeck and Chappell, 2001; Lambeck et al., 2002; Murray-Wallace, 2002; Muhs et al., 2004). In situations where eustatic sea-level change is the main driver of relative sea level, sea-level high stands (henceforth "high stands") can provide important information on changes in polar ice mass and help establish the duration of past interglacials (Gallup et al., 2002: Muhs, 2002). The major Southern Hemisphere landmasses (so-called "far-field" locations) are important for understanding sea-level changes as they have been relatively unaffected by the glacio-hydro-isostatic processes associated with close proximity to waxing and waning ice sheets (Fleming et al., 1998; Bassett et al 2006). They therefore offer the opportunity to reconstruct long-term eustatic and hydro-isostatic sea-level fluctuations where tectonic stability can also be demonstrated (Murray-Wallace, 2002; Woodroffe and Horton, 2005).

Past sea-level high stands have been investigated in various Southern Hemisphere locations (Young et al., 1993; Woodroffe et al., 1995; Stirling et al., 1998; Murray-Wallace, 2002; Tomazelli and Dillenburg, 2007; Hearty et al., 2007; O'Leary et al., 2008). The trailing-edge continental margin of southern South Africa (**Figure 1**) also exhibits an array of marginal marine deposits and associated eolian dune deposits, but most sites currently lack numerical age control. South Africa is a far-field location and the southern Cape coastline is thought to have experienced limited Pleistocene tectonic activity (Goedhart, 2007). As such, emergent evidence of sea-level high stands can provide useful information regarding eustatic sea-level changes and should only be complicated by hydro-isostatic effects (Fleming et al., 1998; Woodroffe and Horton, 2005; Compton, 2001; 2006). Such data also serve to improve our understanding of the

duration of previous interglacial intervals in the southern African context and are relevant to on-going studies at important Middle Stone Age archaeological sites along this coastline (Marean et al. 2007).

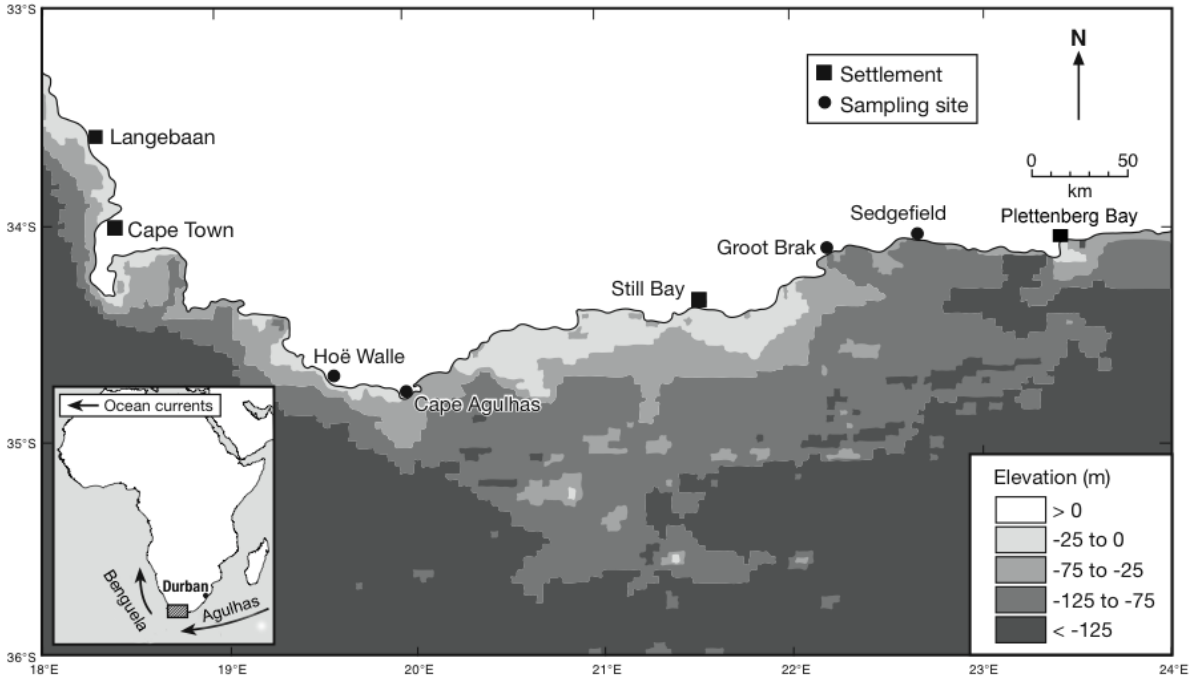

Figure 1: The Southern Cape coastline and continental shelf topography. Sample sites and other sites discussed in the text are marked. Topographic and bathymetric data were derived from the ETOPO v2.2 dataset (U.S. Department of Commerce, 2006) with -125 m representing the approximate last glacial maximum shoreline

The nature and timing of Pleistocene high stands in southern Africa remains contested (Hendy and Volman 1986; Ramsay and Cooper, 2002; Bateman et al., 2004; Butzer, 2004). Several workers have reported evidence for "marine platforms and terraces", which have been identified at various altitudes including 12 m, 8 m, 4.5 m, 2.4 m, 1.4 m, and 1 m above modern sea level (amsl) (Maud 1968), 7-8 m, 4-5 m and 1-2 m amsl (Martin, 1962), 6.3 and 2-3 m amsl (Tankard, 1976), and 12-15, 6-8 and 3 m amsl (Marker, 1987). Such erosional features are, however, extremely difficult to date. A range of emergent marginal marine deposits, for which

geochronological data can now be obtained using luminescence dating techniques, have also been described (e.g., Martin, 1962; Maud 1968; Tankard 1976; Cooper and Flores, 1991; Roberts and Berger, 1997).

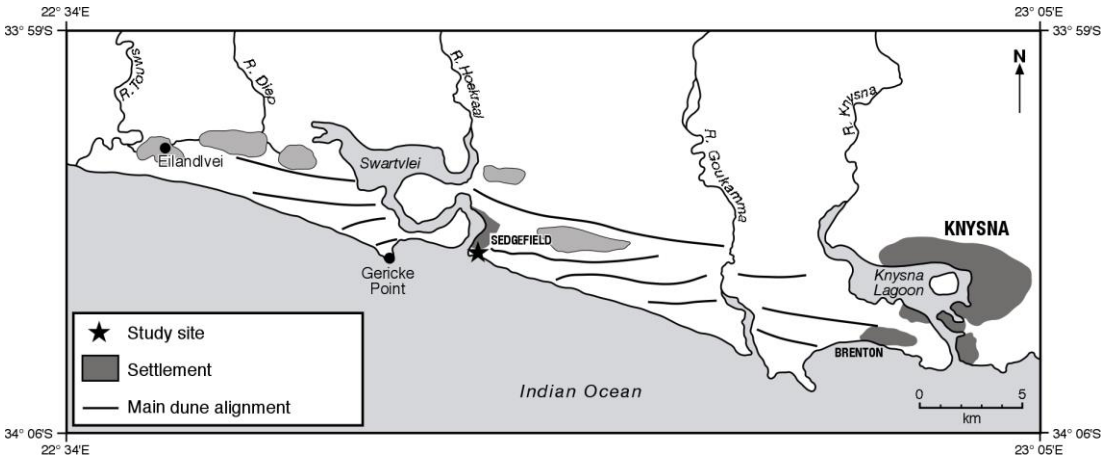

Figure 2: The Wilderness Embayment region, showing the Swartvlei Estuary at Sedgefield and the sampling location

At present, chronological control at most sites, whether erosional or depositional in nature, remains weak or lacking (e.g., Hendey and Volman, 1985). Ramsay and Cooper (2002) presented a discontinuous sea-level curve for South Africa spanning the period 180 ka to the present. Data associated with Marine Isotope Stages (MIS) 5e-5a comprised four uranium-series (U-series) ages in the range 130-100 ka. The uncertainties associated with these ages were variable and large (e.g. 112 ± 23 ka; Pta U415), but they were inferred to post-date MIS 5e (130-116 ka; Kukla, 2000). This was ascribed to reworking during an MIS 5c high stand (ca. 106-95 ka), which was comparable in magnitude (ca. 4 m amsl) to MIS 5e. Such data are inconsistent with other estimates of eustatic sea levels at these times (e.g., Cutler et al., 2003) and the benthic oxygen isotope record (Martinson et al., 1987). They were derived via $^{230}Th/^{234}U$ dating of single mollusk shells; an approach that has been reported to suffer the effects of open-system behavior

93 regarding uranium uptake history (Kaufman et al., 1971; McLaren and Rowe, 1996).
94 Furthermore, mollusks do not precipitate dissolved uranium directly from sea water (Muhs et al.,
95 2004). A fuller suite of dated sea-level high stand indicators is therefore needed to provide a
96 more rigorous consideration of the amplitude and timing of the MIS 5 high stand(s) along the
97 South African coast.

98 The main objective of this study is to refine and extend the South African record of late
99 Quaternary sea-level change through the application of optically stimulated luminescence (OSL)
100 dating at key exposures of raised marginal marine and associated eolian facies. A limited
101 number of amino acid racemization (AAR) analyses provide supplementary relative age
102 constraints. We interpret the resulting ages and amplitudes of paleosea-level fluctuations in
103 relation to the regional coastal geomorphic record and other far-field and eustatic sea-level
104 records.

105

106 *Materials and Methods*

107 We sampled four sites along 300 km of the southern Cape coastline where marginal
108 marine and/or associated eolian sediments are exposed above present sea level (**Figure 1**).
109 Lithology, paleoflow / paleowind patterns and paleontology were used to define the component
110 sedimentary facies. The spatial relationships among the various modern facies were used to
111 derive the depositional setting within the sedimentary record. This permitted the identification of
112 sea-level index points; that is, points of known age, elevation and sea-level tendency (i.e., sea
113 level rising or falling). For each index point the "indicative meaning" is an interpretation of the
114 vertical relationship between the depositional environment of the index point and the
115 contemporaneous mean sea level (Woodroffe and Horton, 2005). The "indicative range" gives an

116 estimated vertical uncertainty in sea level associated with the index point (Ferranti et al., 2006;
117 Woodroffe and Horton, 2005). Although offering the opportunity to apply techniques such as
118 luminescence dating, index points based on beach and foreshore deposits are typically associated
119 with relatively wide indicative ranges (Short, 1984; Ferranti et al., 2006). Elevations of the
120 identified facies and paleosea-level index points relative to modern sea level were obtained via
121 leveling. It is also assumed that past tidal ranges were comparable to the present (i.e., micro-
122 tidal, with a maximum spring range of 1.5-2.0 m; Cooper, 2001).
123
124 ***Sedimentological analyses***
125 Analyses of particle size distribution and calcium carbonate percentage, as well as dry
126 color description, were undertaken (Siesser and Rogers, 1970; Tucker, 1988; Non-affiliated Soil
127 Analysis Working Committee, 1990; Munsell Color, 1994). Particle-size distributions were
128 determined using a settling column. This column, housed at the University of Cape Town,
129 simultaneously measures the sand-sized fraction along with silts and clays. Statistical moments
130 follow the Udden-Wentworth classification (Leeder, 1982) and Folk and Ward (1957)
131 classification. These data are presented in **Table 1.**
132
133 ***Optically stimulated luminescence***
134 OSL dating was conducted at the Sheffield Centre for International Drylands Research
135 (SCIDR; sample codes prefixed "Shfd") and the GeoQuEST Research Centre, University of
136 Wollongong (sample codes UoW-232 to UoW-236). Both laboratories conducted field sampling,
137 equivalent dose and dose-rate measurements independently, thus providing an opportunity to test

the reproducibility of age estimates applied to sediments from the same site using a standard numerical age method.

Samples were obtained by hammering opaque plastic tubes into fresh sediment exposures or by breaking off large blocks of cemented sediment from sections. These blocks were broken up under dim red/orange lighting to extract unexposed sediments. Quartz grains of 150-250 μm (Sheffield) or 180-212 μm (Wollongong) diameters were isolated using standard procedures (Bateman and Catt, 1996; Jacobs et al., 2003). All luminescence measurements were carried out on Risø TL/OSL readers (Bøtter-Jensen et al., 2000) equipped with either blue LEDs (Δ 470 nm; 40 s stimulation) or a filtered (Schott GG420 + SWP interface filters) 150 W halogen lamp (100 s stimulation; samples Shfd05019 and Shfd05047 only). Resulting luminescence signals were detected with EMI 9635Q photomultiplier tubes combined with Hoya U340 filters. Laboratory irradiations were performed by calibrated $^{90}Sr/^{90}Y$ sources.

The single-aliquot regenerative-dose (SAR) protocol (Murray and Wintle, 2000) was used to determine equivalent doses (D_e). Appropriate preheat temperature combinations for regeneration and test doses were determined experimentally via preheat plateau tests and dose recovery experiments (Murray and Wintle, 2003; **table S1**). Growth curves were constructed using between 4 and 7 regeneration points (including a zero dose point) and were fitted using a saturating exponential plus linear equation. Multi-grain D_e values were determined from the first 0.8 s of OSL, using the final 20 s or 8 s as background (for the 100-s and 40-s stimulations, respectively). Tests of protocol performance were made by checking for thermal transfer, test-dose sensitivity correction ('recycling ratio') and the presence of feldspar contamination (Duller, 2003). Aliquots exceeding acceptance thresholds for these tests were removed from the data sets

prior to D_e calculation. D_e uncertainties incorporate an instrumental reproducibility uncertainty of 1%, photomultiplier counting statistics and a growth curve fitting uncertainty.

For each sample, between 12 and 51 aliquots produced acceptable D_e estimates. The resulting D_e distributions were 'overdispersed' by between 4 and 20% (i.e., spread in D_e remaining after known measurement uncertainties have been taken into account; **Table 2 and Figure S1**). Well-bleached, multi-grain aliquots composed of quartz grains may have D_e distributions overdispersed by as much as 20% (Jacobs et al., 2003; Galbraith et al., 2005). Accordingly, we consider that the D_e estimates for all aliquots of each sample record the same depositional event. Thus, weighted mean D_es and standard errors were calculated using the 'central age model' (Galbraith et al., 1999), with an additional uncertainty of 2% associated with laboratory beta-source calibration included for age calculation. The final presented age is accompanied by its 1-sigma uncertainty.

The external beta and gamma dose rates were estimated from the concentrations of uranium (U), thorium (Th) and potassium (K) derived via *in situ* gamma spectrometry, or, where this was not possible, via thick source alpha counting (TSAC; U and Th) and inductively coupled plasma-mass spectrometry (ICP-MS; K; Sheffield); or a combination of TSAC and beta counting (Wollongong). These values were converted to annual dose rates (Adamiec and Aitken, 1998; Marsh et al., 2003), making allowance for beta-dose attenuation (Mejdahl, 1979) and sample water content (Aitken, 1985). In the case of samples deposited within sub-aqueous environments, the modern (measured) water contents, which were as low as 1 %, were considered inappropriate. For these samples time-weighted water content was determined based on the progressive (linear) reduction of water content during burial from a (laboratory-determined) saturated content to the modern value. As an assessment of the sensitivity of sample age to water

content, it is noted that the total dose rate decreases (and optical age increases) by ca. 1% for each 1% increase in water content. An absolute water content uncertainty of ± 5 % was propagated through to the final age determination (Aitken, 1985), which for most samples incorporates a large proportion of the burial history variation in water content.

The agreement between the U and Th concentrations derived by TSAC or gamma spectrometry, and supplementary ICP-MS measurements for samples from two sites suggest that no significant U-series disequilibrium problems are present (**Table S2**). To calculate the optical ages we assumed that the measured radionuclide activities have prevailed throughout the period of burial. Cosmic dose rates were determined following Prescott and Hutton (1994) and modified to account for changing overburden depth through time. This is achieved through the iterative adjustment of the suite of initial (uncorrected) ages in a stratigraphic sequence (see Roberts et al., 2008).

Amino acid racemization (AAR)

AAR allows the determination of the relative age of fossils through the analysis of the D / L ratios of amino acid optical isomers. AAR provided a supplementary means of relative age estimation where OSL sampling was not possible, as well as independent age verification at sites where both techniques were applied. AAR analyses were conducted on marine shells (*Turbo* spp.) and on terrestrial gastropods (*Tropidophora sp.*). The degree of racemization for the amino acids glutamic acid and valine was determined using Reverse Phase High Performance Liquid Chromatography (Kaufman and Manley, 1998). Analyses were undertaken on the total hydrolysable amino acids, after hydrolysis for 22 hours at 110^{o}C in 8 mol HCl. The analytical procedure involved the pre-column derivatization of DL-amino acids with *o*-phthaldialdehyde

206 (OPA) together with the chiral thiol, *N*-isobutyryl-L-cysteine (IBLC) to yield fluorescent
207 diastereomeric derivatives of the chiral primary amino acids. Amino acid D/L ratio
208 determinations were undertaken using an Agilent 1100 HPLC with a C-18 column. These data
209 are presented in **Table 3**.
210

211 ## *Study sites*

212 The southern Cape coastline constitutes a passive intra-plate continental margin. The
213 fragmentation of Gondwanaland initiated a narrow coastal platform seaward of the Great
214 Escarpment, which was subsequently broadened by a series of planation events throughout the
215 Cenozoic (Marker and Holmes, 2005). The region is characterized by a low-gradient continental
216 shelf, which reaches a maximum width of about 130 km south of Still Bay and progressively
217 narrows in an eastwards direction (**Figure 1**). The morphology of the modern coastline east of
218 Cape Agulhas comprises a series of resistant headlands, typically formed from Paleozoic Cape
219 Supergroup quartzites, and sweeping bays mantled by a veneer of Cenozoic marine and eolian
220 sediments.
221

222 ### *Swartvlei Estuary, Sedgefield*

223 The Sedgefield-Wilderness embayment is characterized by a series of shore-parallel
224 "cordons" thought to have formed during multiple Pleistocene sea-level high stands (Illenberger,
225 1996). Martin (1962) described a number of emergent marine deposits along the modern
226 shoreline between Gericke Point and Eilandvlei (**Figure 2**). These were reported to reach a
227 maximum altitude of 7.5 m amsl. We were unable to relocate these exposures in the field and

instead report a stratigraphic succession exposed at the mouth of the Swartvlei Estuary about 5 km farther east.

Two sections 30 m apart were examined. In both sections the basal facies (from 0 m amsl) comprises 0.5-1.0 m (lower contact not exposed) of medium to coarse grained, well-sorted, structureless calcarenite (**Figure 3**). The transition from this lower unit to the overlying facies is notably disconformable and marked by rip-up clasts. This lower unit was apparently lithified and partially reworked (forming a transgressive lag) prior to the deposition of the overlying facies (**Figure S2**).

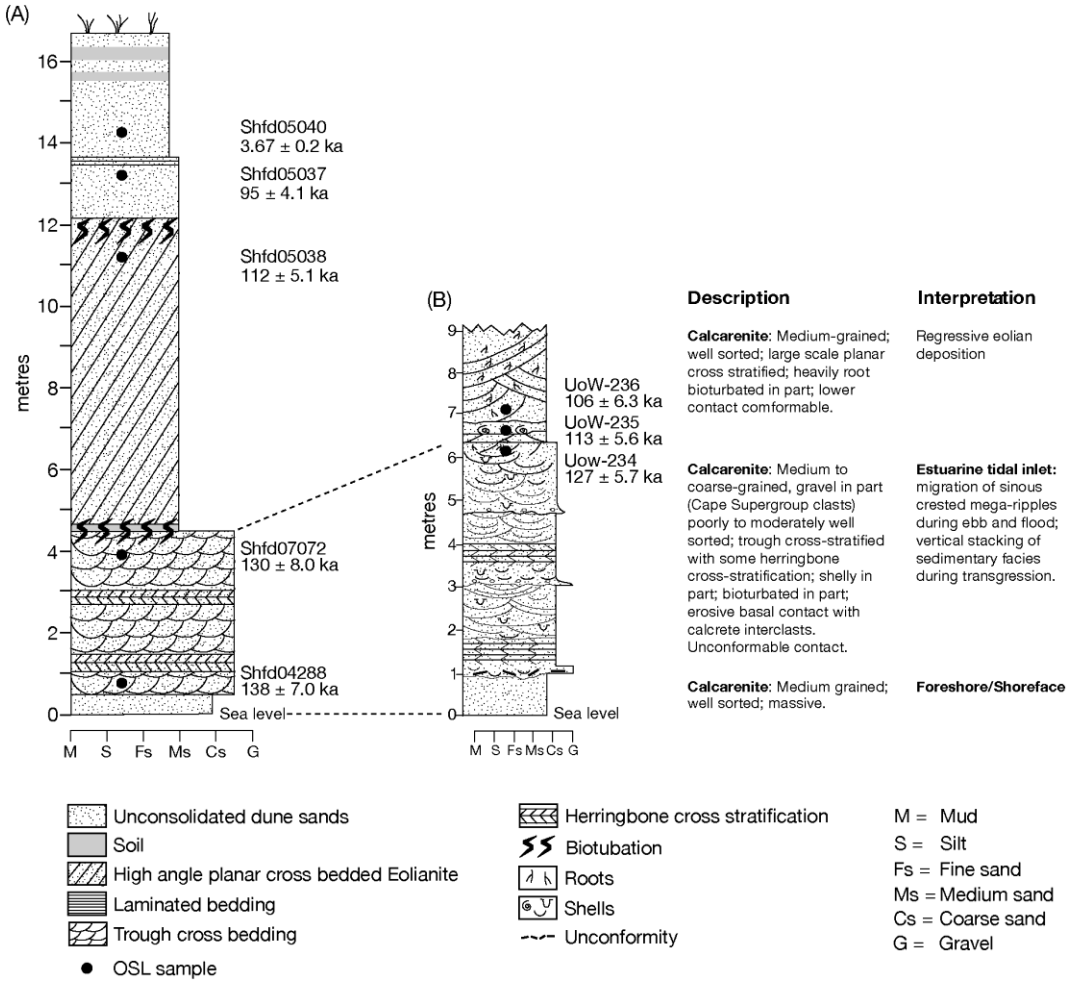

Figure 3: The Swartvlei Estuary sample site. (A) Stratigraphy of primary site (B) detailed stratigraphy of the estuarine inlet facies from offset section, showing OSL samples UoW-234, UoW-235 andUoW-236.

239 Overlying this from 0.5 - 1.0 m amsl up to 5.6 m amsl is a very coarse-grained,
240 moderately sorted, thickly bedded calcarenite, structured by trough cross-bedding and, less-
241 commonly, herringbone cross-bedding (**Figure 3; Figure S3**). The strata contain marine
242 mollusks, including limpets (*Patella* sp.) and cockles (Cardiidae) as well as vertical burrows of
243 the ichnogenera *Skolithos* and *Ophiomorpha* (e.g. Tomazelli and Dillenburg, 2007). Numerous
244 internal scours mantled by coarse, occasionally gravelly, detritus are observed. This facies
245 reaches 4.8 m amsl section A, but is slightly thicker (5.6 m amsl) in section B (**Figure 3B**). The
246 lithology and sedimentary structures of this facies are indicative of a tidal inlet environment and
247 suggest a setting dominated by the uni- and bidirectional migration of sub-aqueous mega-ripples,
248 giving rise to the trough and herringbone cross bedding (Reddering, 1983; Massari and Parea,
249 1988). This interpretation is analogous to the existing tidal inlet of the Swartvlei Estuary. The
250 indications of reversing currents within erosional scours are compatible with deposition in
251 migrating tidal channels (scour and fill). Generally, the contact with the overlying eolianite
252 facies at 4.5 – 5.6 m amsl appears conformable, although a coarse shelly (possibly deflationary)
253 lag is sporadically exposed. The overlying eolianite facies displays high-angle planar cross-
254 bedding typical of Pleistocene dunes in this region. Eight OSL samples, encompassing three
255 samples from the inlet facies and five samples from the eolianite were obtained from this site.
256
257 ***Groot Brak Estuary***
258 65 km west of Sedgefield, calcified shallow marine and eolian sediments are exposed on
259 the banks of the Groot Brak Estuary (**Figures 1 and 4**). This succession is exposed/partially
260 exposed up to 450 m inland of the estuary mouth, whereupon it becomes inaccessible for study
261 due to the terrain and vegetation. The succession comprises a lower facies (0-1.0 m amsl) of

Final version available at http://www.sciencedirect.com/science/article/pii/S0033589409001112

medium grained, massive calcarenite, overlain by moderately-sorted, coarse-grained, shelly calcarenites, grading to gravel in places (1.0 - 4.9 m amsl). Trough cross-stratification is the dominant sedimentary structure in the latter facies, along with occasional herringbone cross-stratification. This bears close similarities with the exposure at the Swartvlei Estuary and is interpreted similarly.

This facies is conformably overlain by well sorted, gently seaward and landward dipping low-angle cross-stratified calcarenites, which reach up to 9.8 m amsl. This low-angle cross-stratified facies is interpreted as a beach berm swash deposit (Reddering, 1983; Short, 1984), modern analogues of which form on the banks of the contemporary estuary. Today these are usually the product of storms or spring high tides and are observed to reach up to 2 m above the tidal channel. This beach berm facies is conformably overlain by high-angle cross-stratified eolianites. OSL samples were obtained from the base of the beach berm facies (9.0 m amsl) and from the base of the overlying eolianite (10.5 m amsl).

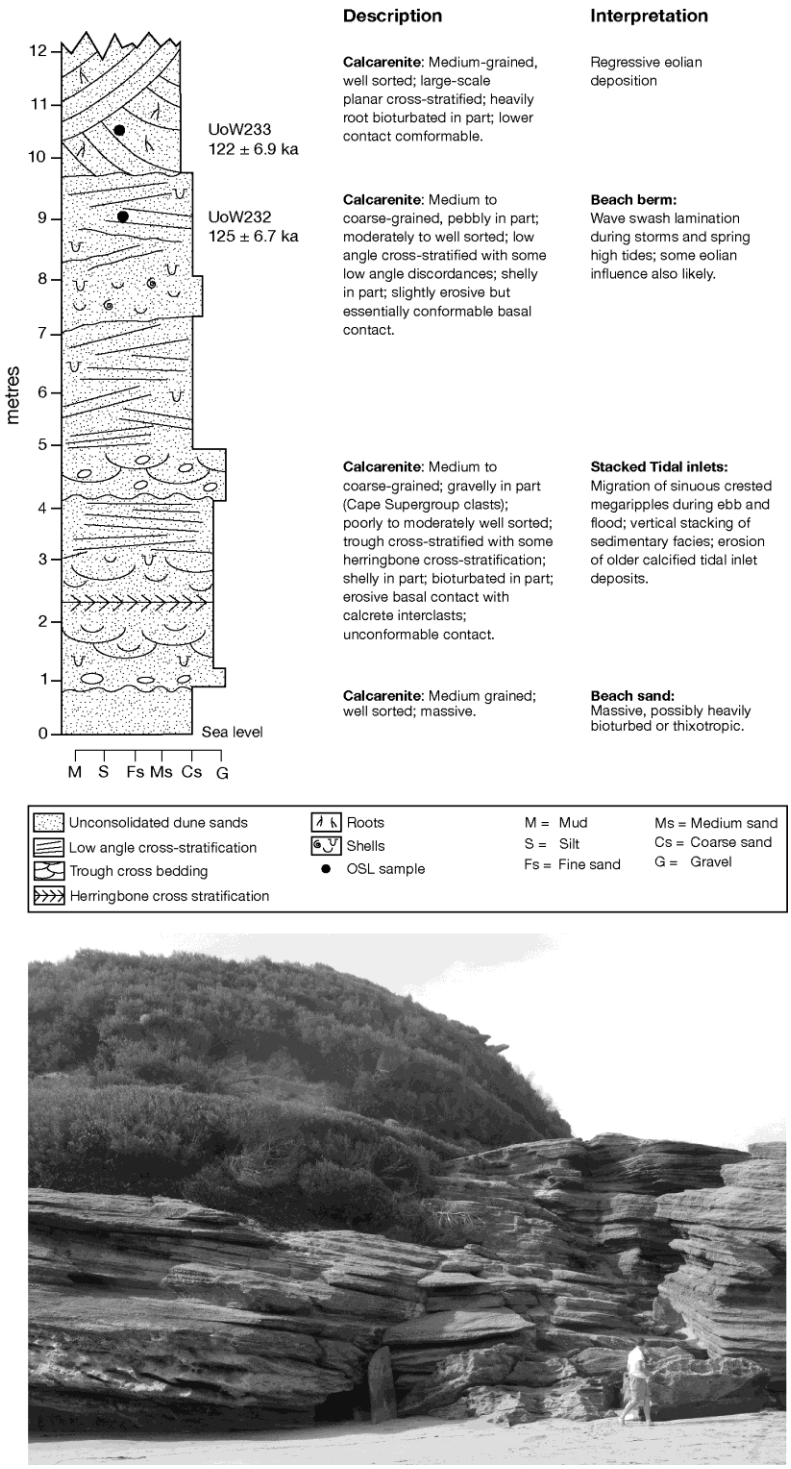

Figure 4: Upper: the stratigraphic log for the Groot Brak Estuary site with OSL samples marked. See figure 3 legend for log symbols. Lower: view of the sample site showing the low angle cross stratified beach berm facies.

Final version available at http://www.sciencedirect.com/science/article/pii/S0033589409001112

Cape Agulhas

Two sites in the Cape Agulhas area display evidence pertinent to palaeosea-level fluctuations (**Figure 5**). Northeast of Cape Agulhas, a raised beach deposit with a basal altitude of 3.0 m amsl is exposed landward of the modern rocky shoreline. The lower part of the section (**Figure 6**) comprises a ca. 0.8-m-thick unit (basal contact not exposed) composed of tightly-packed and well-rounded clasts of quartzite (long axis 0.1-0.5 m) and includes the marine mollusks *Turbo* sp. and *Patella* sp. The faunal remains and lithology are indicative of a rocky shoreline comparable to the present setting. This gravel beach facies is unconformably overlain by a 3.9 m thick deposit of structureless sands composed mostly of comminuted shell (ca. 84 % carbonate by mass). The lithology and grain size parameters of these sands (mean 1.1ø; sorting 0.36; skewness 0.11), contrast sharply with nearby eolianites (**Table 1**) and the former are interpreted as a wave winnowed foreshore deposit. These calcareous sands grade upwards into a pedogenic calcrete, capped by a well-developed laminated hardpan at 7.6 m amsl, which is in turn overlain by a modern soil. An OSL sample was obtained from these foreshore sands at 5.6 m amsl.

Further sampling was carried out in the eroding backshore cliffs at Hoë Walle, west of Cape Agulhas (Malan, 1990; Bateman et al., 2004; **Figure 5)**. The lower part of the section (0 - 4.5 m amsl) comprises structureless, uncemented calcareous sands within which three paleosols of variable maturity are preserved. The most mature paleosol (paleosol 2; **Figure 7**) lies at 4.5 m amsl, and predates 88 ± 4 ka (Shfd02131; Bateman et al., 2004). In this study an additional OSL sample was obtained from a structureless sandy unit at 4 m amsl, 0.5 m below paleosol 2. In addition, a specimen of the terrestrial gastropod *Trophidophera sp.* was obtained from the underlying paleosol 3 at 3.4 m amsl.

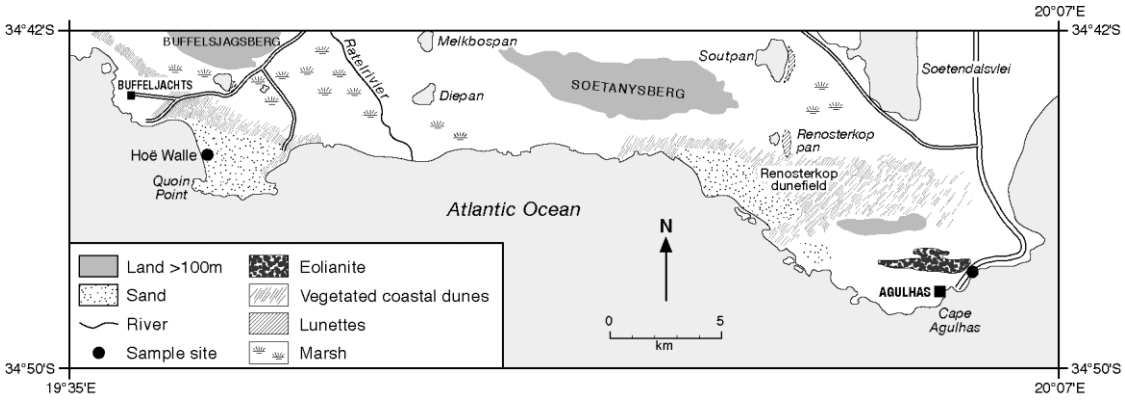

304

305 Figure 5: Sampling locations in the Cape Agulhas area

306

307 ## *Geochronological Results*

308 ### *Swartvlei Estuary*

309 Eight OSL samples were obtained from the Swartvlei Eustary (**Figure 3 and Table 2**).
310 Three were collected from the tidal inlet facies (UoW-234, Shfd07072 and Shfd04288), and five
311 from the overlying eolian facies (samples Shfd05038-05040, UoW-235 and UoW-236). Sample
312 Shfd04288 (138 ± 7 ka) provides a basal age for the tidal inlet facies (1 m amsl). The distinct
313 lithofacies sequence at the site enabled easy correlation between the two measured sections, with
314 UoW-234 and Shfd07072 both corresponding with the top of the tidal inlet facies (127 ± 6 ka
315 and 130 ± 8 ka respectively). The eolianite immediately overlying the inlet facies produced OSL
316 ages of 113 ± 6 ka (UoW-235) and 106 ± 6 ka (UoW-236). Remaining ages from the eolianite
317 were 112 ± 5 ka, (Shfd05038) and 95 ± 4 ka (Shfd05039); with the overlying Holocene dune
318 sands dating to 3.67 ± 0.2 ka (Shfd05040). The stratigraphic concordance of the eight ages
319 derived from this site, which were sampled and measured independently at Sheffield and
320 Wollongong, provides additional confidence in this chronology.

321

Final version available at http://www.sciencedirect.com/science/article/pii/S0033589409001112

322 ***Groot Brak Estuary***

323 OSL ages of 125 ± 7 ka (UoW-232) and 122 ± 7 ka (UoW-233) were obtained for the
324 samples from the beach berm and eolianite facies respectively (**Table 2; Figure 4).** Like the
325 Swartvlei Estuary site, these ages are stratigraphically concordant and the facies relations at the
326 two sites are comparable; the similarity in ages provides further confidence in these data.

327

328 ***Cape Agulhas***

329 The sample from the coarse sand deposits at 5.6 m amsl (Shfd05019; **Figure 6**) produced
330 an OSL age of 118 ± 7.2 ka (**Table 2**). This sample has the highest D_e overdispersion in our data
331 set (20%; **Figure S1**). This over-dispersion is not excessive (Jacobs et al., 2003), and the
332 equivalent dose distribution, although relatively broad, is not strongly skewed. Two specimens of
333 *Turbo* sp. were sampled from the raised gravel beach facies for AAR analysis (**Table 3**). The
334 degree of racemization of valine ranged from 0.35 (UWGA5232A-F) to 0.41 (UWGA5233A-C),
335 with glutamic acid showing slightly higher D/L values of 0.41 (UWGA5232A-F) and 0.46
336 (UWGA5233A-C). An operculum from a further specimen of *Turbo* sp. yielded a minimum
337 radiocarbon age of >36,244 ^{14}C yr BP (Wk-19265).

338

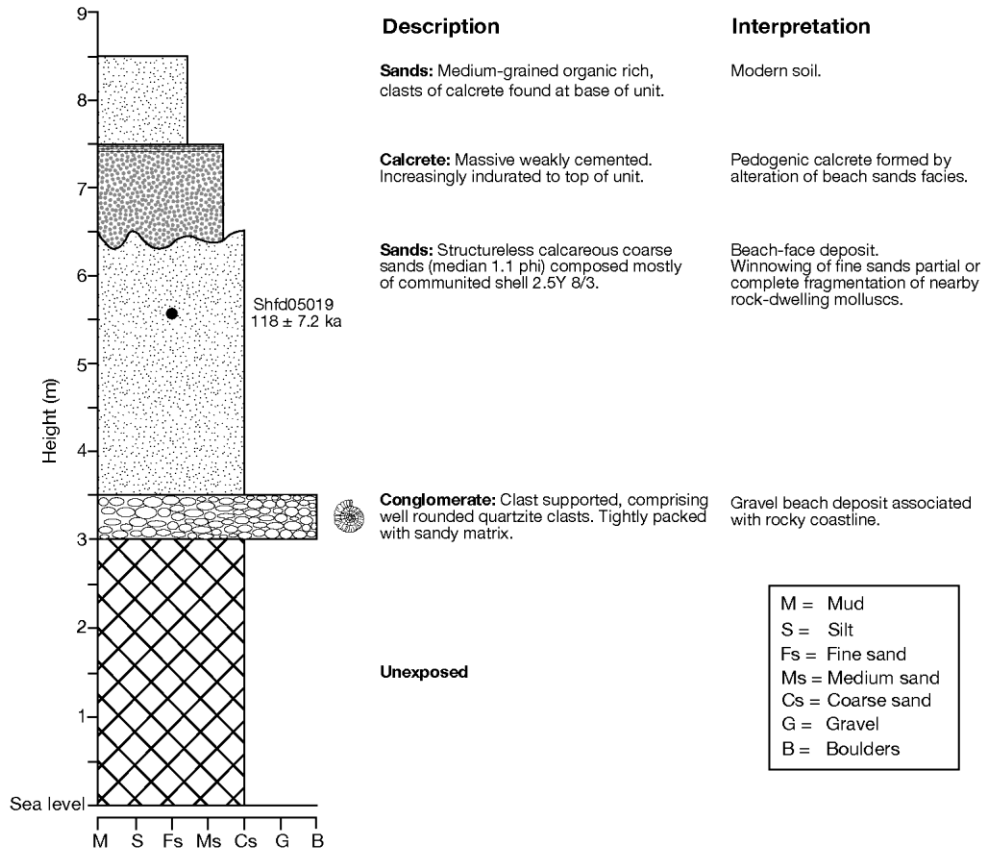

Figure 6: The stratigraphic section for the raised beach at Cape Agulhas. A photograph of the raised gravel beach deposit is also shown below. Geological hammer center-left for scale.

342 At Hoë Walle an OSL age of 104 ± 7 ka (Shfd05047) was obtained for the sample 0.5 m
343 below paleosol 2 (4.5 m amsl). This is stratigraphically consistent with published OSL ages from
344 this site (Bateman et al., 2004; **Figure 7**) and brackets the formation of paleosol 2 to < 104 ± 7
345 ka and > 88 ± 4 ka. AAR data for the terrestrial gastropod sampled from paleosol 3 (3.4 m amsl)
346 reveal a lower degree of racemization (D/L ratios of 0.274 ± 0.019 and 0.373 ± 0.022 for valine
347 and glutamic acid respectively; **Table 3**) than MIS 5e gastropods elsewhere on this coastline
348 (Roberts et al. 2008; valine 0.379 ± 0.103; glutamic acid 0.576 ± 0.075; UWGA5225A-C),
349 lending further support to the OSL ages and the inference that that this sequence post dates the
350 last interglacial (MIS 5e; 130-116 ka).
351

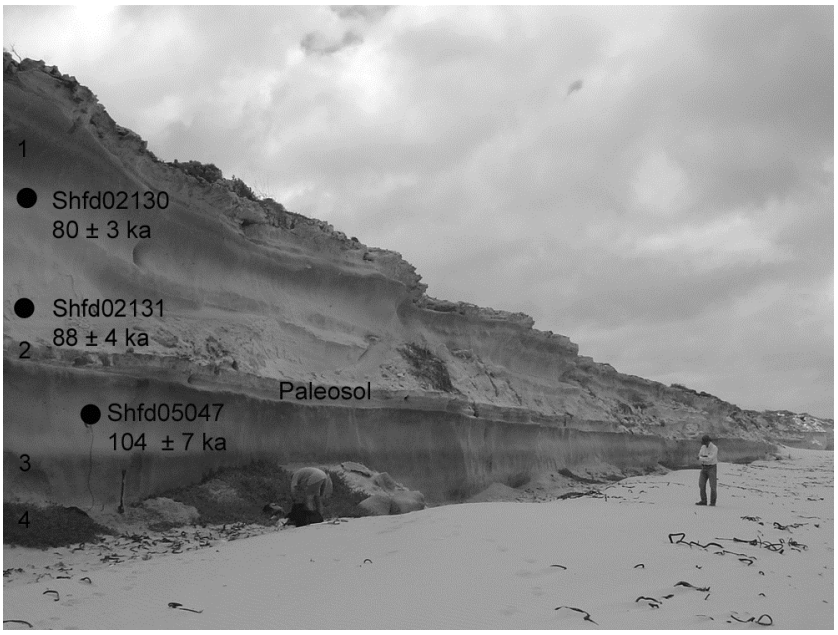

352
353 Figure 7: The sample site at Hoë Walle. Sample locations and ages reported in Bateman et al (2004) are marked, as
354 is the current sample. Four paleosols identified at this site are numbered. The most prominent paleosol (2) comprises
355 indurated planar laminated silty sands. Diffuse paleosols (3 and 4) are marked by slight organic matter enrichment
356 and loss of bedding structure. A specimen of the dune snail *Trophidophera sp.* was sampled from paleosol 3.
357

Discussion

Evidence of sea-level change

Our data provide numerical age assessments for high stands at 3 localities along the southern Cape coastline, along with new chronologies for associated coastal eolian activity. Both of the successions at the Swartvlei and Groot Brak estuaries are interpreted as essentially regressive in character (e.g., Cooper and Flores, 1991). At Swartvlei, sea-level index points are provided by OSL ages Shfd04288 and Shfd07072 / UoW-234 for the base and top (respectively) of the tidal inlet facies. The former provides a minimum age of 138 ± 7 ka (Shfd04288) for the sea-level transgression that partially reworked the lowermost (0-1.0 m amsl) calcarenite facies. A rising sea-level trend inundating subaerially exposed sediment is inferred for this period.

A second sea-level index point representing the maximum sea level recorded at this site is provided by OSL sample UoW-234 (127 ± 6 ka), which was obtained at 5.6 m amsl. Given that it is immediately overlain by unequivocally eolian facies the index point at 5.6 m amsl is associated with the initiation of a regressive sea-level trend. The precise indicative meaning of this index point is complicated by the overall seaward dip of the exposed strata. The maximum landwards extent of the inlet/eolian facies change is not exposed and the index point of 5.6 m amsl must be treated as a minimum palaeosea-level estimate. Given that the angle of dip is low (1-2^{o}) the index point is unlikely to rise much higher, which we estimate to be no more than ca. 1 m. (i.e., 6.6 m amsl). The indicative meaning of this index point must also account for the water depths in which the characteristic tidal inlet facies form. Reddering (1983) provides a detailed overview of a wave-dominated micro-tidal inlet at Plettenberg Bay (**Figure 1**). Here, trough cross-bedded flood tide inlet facies, comparable to those at Swartvlei are currently deposited 0.5 – 3.5 m below the mean water level. Given similar water depths in the contemporary inlet at

Swartvlei we infer an indicative meaning of ca. 8.5 m amsl for this index point, which accounts for both the dip of the strata and the probable depositional environment of the inlet facies. The presence of the inchnogenera *Ophiomorpha* and *Skolithos* throughout the inlet facies, which have been associated with sediments close to the average low tide level and water depths less than 5 m, supports this interpretation (Frey et al., 1978; Tomazelli and Dillenburg, 2007). Notwithstanding, estuaries/inlets along the southern Cape coastline are characterized by considerable morphological dynamism (Reddering, 1983; Cooper, 2001) and so an associated indicative range of ± 2 m is applied **(Table 4)**.

At Groot Brak Estuary the tidal inlet facies reaches an altitude of 4.9 m amsl. However, like Swartvlei these exhibit a very low seawards dip (<1^{o}), which can be projected inland to ca. 7.3 m amsl. The OSL sample (125 ± 7 ka; UoW-232) obtained from beach berm facies at 9 m amsl provides an index point marking a regressive sea-level trend (transition from beach berm to eolian facies). It also provides a minimum age for the inlet facies. The contact between the inlet facies and beach berm facies is conformable, and this OSL age is likely to broadly reflect the age of the former. Modern analogues for the beach berm facies are deposited up to 2 m amsl, implying an indicative meaning of ca. 7.0 m amsl for the index point. However, swash-formed deposits are associated with relative wide indicative ranges (Reddering, 1983; Ferranti et al., 2006), which we estimate as ± 3 m. Given a maximum exposed altitude of 9.8 m amsl, a maximum paleosea level in the region of 7.8 m amsl is inferred for the beach berm facies. This is consistent with the maximum sea level inferred from the inlet facies and with interpretations at Swartvlei.

At Cape Agulhas the foreshore deposit dated by OSL provides a sea-level index point at 5.6 ± 3 m amsl (118 ± 7 ka; Shfd05019). This is associated with a relatively large indicative

range (**Table 4**), which reflects the unknown affects of degradation during the very evident pedogenesis at this site, possible damage from road construction above the sample site, and more fundamentally the wide indicative range inherently associated with sandy foreshore deposits (Short, 1984; Ferranti et al., 2006). The site stratigraphy implies, with the noted caveats, that sea level may have reached as high as ca. 7.5 m amsl (**Figure 6**). Constraining the absolute age of the gravel beach facies is difficult as there are few age-calibrated AAR data for southern African *Turbo* specimens. The Cape Agulhas specimens display a significantly higher degree of racemization than a mid-Holocene *Turbo cidaris* specimen from the same area (0.187 ± 0.018; **Table 3**; Bateman et al., 2008).

A survey of the degree of racemization in a wide range of molluscan fossil genera of late Pleistocene age from southern Australia (although not including *Turbo*) suggests that the Cape Agulhas *Turbo* sp. shells are significantly older than the minimum radiocarbon age, assuming that comparable modern mean annual temperatures imply, as corollary, comparable diagenetic temperatures (Murray-Wallace, 2000). The depositional setting and the degree of racemization of glutamic acid and valine in the *Turbo* specimen support the assumption that the *Turbo* sp. shells are broadly contemporaneous with the overlying sands (118 ± 7 ka), and that the true age of the *Turbo* sp. specimens is significantly greater than the minimum radiocarbon age.

Overall, the geomorphic evidence at Cape Agulhas also implies two distinct sea-level phases; initially a gravel beach at 3.0-3.8 m amsl, with a subsequent sandy foreshore deposit reaching ca. 7.5 m amsl. This distinct shift in depositional environment probably reflects an adjustment in wave energies around the headland as the shoreline reconfigured.

The OSL ages from Hoë Walle provide sea-level limiting points (i.e., maximum possible sea levels), as sea level must have been lower than the sampled altitude to allow eolian sand

transport and subsequent soil (paleosol) development. Thus, the OSL ages at this site suggest landscape stability (soil formation) and sea levels probably lower than 4 m amsl throughout the period ca. 111-77 ka (maximum and minimum ages, incorporating 1 sigma uncertainties for the OSL samples bracketing paleosol 2).

The generally conformable interface between the inlet/beach berm and eolianite facies at Swartvlei and Groot Brak implies a limited pause in sedimentation (only a minor deflationary lag is evident at Swartvlei) before the initiation of eolian activity, determined via OSL to have occurred during the period 122 ± 7 ka (UoW-233) to 113 ± 6 ka (UoW-235). However, it is difficult to ascertain the extent to which the sampled regressional sequences also record coastal progradation due to increased sediment supply. In the case of the Wilderness and Still Bay regions, the formation of extensive barriers ("cordons") throughout MIS 5 (ca. 130-70 ka) reflects the delivery of large volumes of sediment to the region's beaches. The spread of eolianite OSL ages in this study is consistent with the regional record of eolian activity along this coastline, which indicates that dune accumulation remained high throughout and subsequent to MIS 5e before diminishing towards the MIS 5a/4 transition (Carr et al., 2007; Roberts et al., 2008; Roberts et al 2009). In contrast with evidence elsewhere in the Wilderness dune cordons (Carr et al., 2007), the Swartvlei Estuary site does not record eolian deposition at the height of MIS 5e, probably reflecting the flooding of this sector of the Wilderness Embayment.

Wider significance

With consideration of the age uncertainties, all of the marginal marine / inlet facies provide ages consistent with MIS 5e and reveal that sea levels comparable to or above present were attained between 138 ± 7 ka (Shfd04288) and 118 ± 7 ka (Shfd05019). These broadly

accord with expected timing of MIS 5e from the benthic oxygen isotope record (130-117 ka; e.g. Martinson et al., 1987; Lisiecki and Raymo, 2005), as well as Waelbroeck et al.'s (2008) recent estimate for the onset of the MIS 5e high stand (126 ± 1.7 ka) based on coral reef data from a range of near and far-field locations (Bahamas, Hawaii and Western Australia). The evidence of two phases of higher sea level at Cape Agulhas also accords with the recent arguments of Hearty et al. (2007). The OSL ages from the near the top of the Agulhas site (118 ± 7 ka), the lowermost eolianite at the Swartvlei Estuary (113 ± 6 ka), and the Groot Brak eolianite (122 ± 7 ka) are broadly consistent (given uncertainties) with the expected timing of the MIS 5e/5d sea-level regression ca. 118 - 115 ka (Stirling et al. 1998; Speed and Cheng 2004; Hearty et al., 2007), as well as the marine oxygen isotope record (Martinson et al., 1987). In contrast to the interpretation of Ramsay and Cooper (2002), none of the southern Cape inlet or shoreface facies produced an age equivalent to MIS 5c (beginning ca. 106 ka; Kukla, 2000). Ramsay and Cooper's (2002) interpretation was based on U-series ages of 104.9 ± 9 ka (Pta-U568) and 95.7 ± 4.2 ka (Pta-U565) from oyster specimens. At present, such an interpretation is not supported by coral reef evidence (e.g., Cutler et al., 2003; MIS 5c sea levels between -14 ± 3 m and -10 ± 3 m) or the marine oxygen isotope stratigraphy (Martinson et a1., 1987; Waelbroeck et al., 2002; **Figure 8**).

Figure 8 summarizes the new sea-level data from the southern Cape and the timing of associated eolian activity. Overall, our data confirm sea levels significantly higher than the present along the southern Cape coastline during MIS 5e, and a 6-8.5 m amsl maximum high stand is inferred (**Table 4).** This is comparable with (undated) 5-7 m amsl shoreline deposits near Durban (Cooper and Flores, 1991), as well as repeated reports of marine benches and terraces between 5 and 8 m amsl elsewhere on the South African coastline (e.g., Maud, 1968; Tankard,

1976; Marker 1987). In general, these data are also consistent with MIS 5e eustatic sea-level estimates from a range of Southern Hemisphere passive margin locations, including southern Brazil (7 m amsl; Tomazelli and Dillenburg, 2007) and Western Australia (4-10 m amsl, with two distinct terraces/sea levels inferred by Hearty et al. 2007 and O'Leary et al., 2008; [see also Stirling et al., 1995, 1998]). They are also comparable to data reported for Florida (5-8 m amsl; Muhs et al., 2004). They are generally higher than estimates from southern Australia (2-6 m amsl; Murray-Wallace, 2002), particularly the Eyre Peninsula (ca. 2 m amsl; Murray-Wallace and Belperio, 1991).

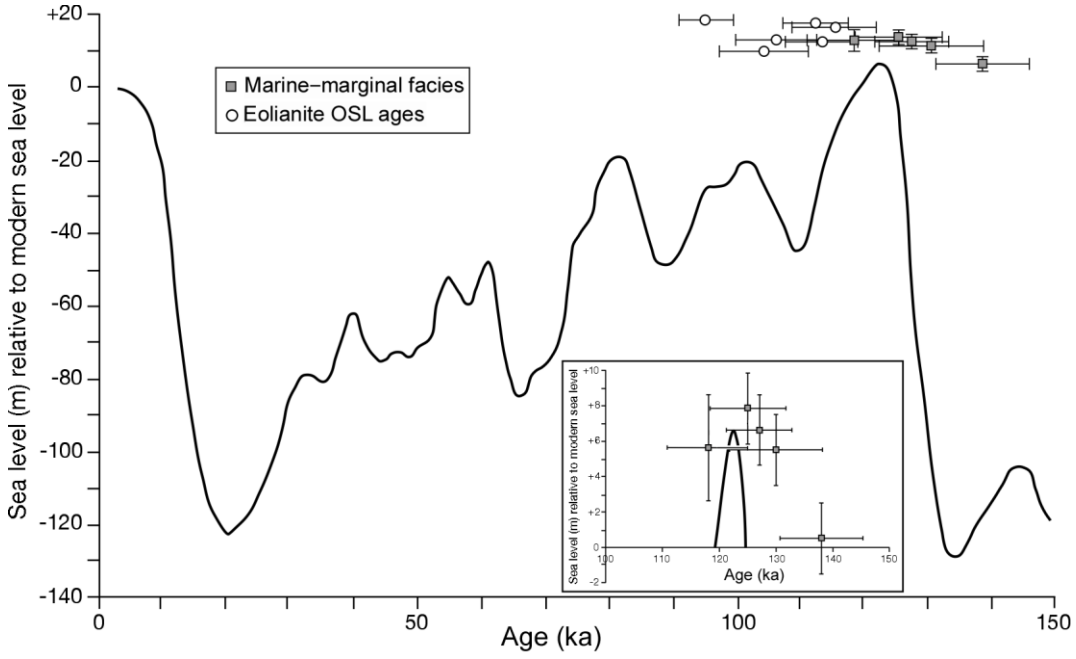

Figure 8: The timing of eolianite and marine-marginal sedimentation on the southern Cape coastline in relation to the sea-level curve of Waelbroeck et al. (2002). Inset: indicative meanings and ranges for the marine-marginal facies sampled at Swartvlei Estuary, Groot Brak Estuary and Cape Agulhas.

If assumed to primarily reflect eustatic sea-level change, a highstand of ca. 6-8.5 m amsl would support the hypothesis that melting of the Greenland ice sheet alone could not have accounted for the MIS 5e sea-level high stand (e.g., Overpeck et al., 2006; Hearty et al., 2007).

However, Holocene sea-level records on the west coast of South Africa (Baxter and Meadows, 1999; Compton, 2001) and Namibia (Compton, 2006) demonstrate the existence of a ca. 2-3 m amsl high stand ca. 7300-6500 cal yr BP, which is thought to primarily reflect hydro-isostatic sea-level fluctuations (Compton, 2006). The extent to which these processes affected the southern Cape during MIS 5e is difficult to ascertain. Hearty et al (2007) recently noted the consistency of last interglacial sea-level records from both far-field (Australia) and intermediate-field (e.g., Bermuda) locations, despite their theoretically different hydro-isostatic responses during high stands. A eustatic interpretation of the present data also assumes no tectonically-induced changes in relative sea level. Although supported by the passive margin tectonic setting of the southern Cape, regional uplift or subsidence of this section of coastline during the last ca. 140 ka cannot be completely ruled out on the basis of these data.

Conclusions

This paper provides evidence for sea-level fluctuations on the south coast of South Africa during the last 140 ka and suggests a 6-8.5 m amsl sea-level high stand concordant in timing with Marine Isotope Stage 5e. The sample sites at the Swartvlei and Groot Brak Estuaries reveal essentially regressive sequences, with tidal inlet facies presently exposed up to 5.6 m amsl. OSL ages from the overlying eolianite imply a significant sea-level regression and/or coastline progradation ca. 122 ± 7 ka - 113 ± 6 ka. At Cape Agulhas, evidence for two phases of high sea level is preserved, recording a shift from a rocky shoreline comparable to the present, to a sandy shoreline up to 7.5 m amsl. An OSL age of 118 ± 7 ka was been obtained for this final phase. Overall, these data support the view that sea-level fluctuations on the southern Cape of South Africa broadly mirror eustatic sea-level changes in far-field / Southern Hemisphere sites.

However, the absolute magnitude of the high stand is greater than that recorded in some locations and at present isolating the impact of hydro-isostatic effects is difficult.

Acknowledgements

This research was partially funded by the Leverhulme Trust (F/00 118/AF). South African National Parks are thanked for granting permission to work in the Wilderness National Park. Transport and accommodation were funded by the University of the Free State. Paul Coles and Gail Holmes are thanked for cartographic assistance and sedimentological analyses respectively. The South African power utility Eskom is acknowledged for permission to publish confidential data. Claire Waelbroeck is thanked for providing the sea-level data used in figure 8. This paper benefited from the constructive comments of Dan Muhs, John Compton and an anonymous reviewer.

References

Adamiec G., Aitken M.J. 1998. Dose-rate conversion factors: update. Ancient TL 16, 37-50

Aitken, M. J. 1985. Thermoluminescence Dating. Academic Press, London.

Bassett, S.E., Milne, G.A., Mitrovica, J.X., Clark, P.U. 2005. Ice Sheet and solid Earth influences on Far-Field sea-level histories. Science 309, 925-928.

Bateman, M.D., Catt, J.A. 1996. An absolute chronology for the raised beach deposits at Sewerby, East Yorkshire, U.K. Journal of Quaternary Science 11, 38-395.

Bateman, M.D., Holmes, P.J., Carr, A.S., Horton, B.P., Jaiswal, M.K. 2004. Aeolianite and barrier dune construction spanning the last two glacial-interglacial cycles from the southern Cape coast, South Africa. Quaternary Science Reviews 23, 1681-1698.

Final version available at http://www.sciencedirect.com/science/article/pii/S0033589409001112

535 Bateman, M.D., Carr, A.S., Murray-Wallace, C.V., Holmes, P.J., Roberts, D.L. 2008. A dating
536 inter-comparison study on Late Stone Age Midden deposits, South Africa.
537 Geoarchaeology 23, 715-741
538 Bard, E., Hamelin, B., Fairbanks, R.G., 1990, U-Th ages obtained by mass spectrometry in
539 corals from Barbados: Sea-level during the past 130,000 years. Nature 346, 456–458.
540 Baxter, A.J., Meadows, M.E. 1999 Evidence for Holocene sea-level change at Verlorenvlei,
541 Western Cape, South Africa. Quaternary International 56, 65-79
542 Bøtter-Jensen, L., Bulur, E., Duller, G.A.T., Murray, A.S., 2000. Advances in luminescence
543 instrument systems. Radiation Measurements 32, 523-528.
544 Butzer, K.W. 2004. Coastal eolian sands, paleosols, and Pleistocene geoarchaeology of the
545 Southwestern Cape, South Africa. Journal of Archaeological Science 31, 1743-1781
546 Carr, A.S., Bateman, M.D., Holmes, P.J. 2007. Developing a 150 ka luminescence chronology
547 for the coastal dunes of the southern Cape, South Africa. Quaternary Geochronology 2,
548 110-116
549 Compton, J.S. 2001. Holocene sea-level fluctuations inferred from the evolution of depositional
550 environments of the southern Langebaan Lagoon salt marsh, South Africa. The Holocene
551 11, 395–405
552 Compton, J.S. 2006 The mid-Holocene sea-level highstand at Bogenfels Pan on the southwest
553 coast of Namibia. Quaternary Research 66, 303-310
554 Cooper, J.A.G. 2001. Geomorphological variability among microtidal estuaries from the wave-
555 dominated South African coast. Geomorphology 40, 99-122.

556 Cooper, J.A.G., Flores, R.M. 1991. Shoreline deposits and diagenesis resulting from two Late
557 Pleistocene highstands near +5 and + 6 metres, Durban, South Africa. Marine Geology
558 97, 325-343.
559 Cutler, K.B. Edwards, R.L. Taylor, F.W. Cheng, H. Adkins, J. Gallup, C.D. Cutler, P.M. Burr
560 G.S. Bloom A.L. 2003. Rapid sea-level fall and deep-ocean temperature change since the
561 last interglacial period. Earth and Planetary Science Letters 206, 253-271
562 Duller, G.A.T., 2003. Distinguishing quartz and feldspar in single grain luminescence
563 measurements. Radiation Measurements, 37, 161-165.
564 Ferranti, L., Antonioli, F., Mauz, B., Amorosi, A., Dai Pra G., Mastronuzzi, G., Monaco, C.,
565 Orrù, P., Pappalardo, M., Radtke, U., Renda, P., Romano, P., Sansò, P. and Verrubbi, V.
566 2006. Markers of the last interglacial sea-level highstand along the coast of Italy: tectonic
567 implications. Quaternary International 145-146, 30-54
568 Fleming, K., Johnston, P., Zwartz, D., Yokoyama, Y., Lambeck, K., Chappell, J. 1998. Refining
569 the eustatic sea-level curve since the Last Glacial Maximum using far- and intermediate-
570 field sites. Earth and Planetary Science Letters 163, 327-342
571 Folk, R.L., Ward, W.C., 1957. Brazos River Bar, a study in the significance of grain size
572 parameters. Journal of Sedimentary Petrology 27, 3-26.
573 Frey, R.W., Howard, J.D., Pryor, W.A. 1978. Ophiomorpha — its morphologic, taxonomic, and
574 environmental significance, Paleogeography Palaeoclimatology Palaeoecology 23, 199–
575 229
576 Galbraith, R. F., Roberts, R.G., Laslett, G.M., Yoshida H., Olley, J.M. 1999. Optical dating of
577 single and multiple grains of quartz from Jinmium rock shelter, northern Australia, part 1,
578 Experimental design and statistical models. Archaeometry 41, 339-364.

Galbraith, R.F., Roberts, R.G. & Yoshida, H. 2005. Error variation in OSL palaeodose estimates from single aliquots of quartz: a factorial experiment. Radiation Measurements 39, 289–307.

Gallup, C.D., Cheng, H., Taylor, F.W., Edwards, R.L. 2002. Direct determination of the timing of sea level change during Termination II. Science 295, 310–313

Goedhart, M. 2007. Seismicity along the southern Cape Fold Belt, South Africa, association with geological structures, and early Holocene reactivation of the Kango Fault. Quaternary International 167-168, 142.

Hearty, P.J., Hollin, J.T., Neumann, A.C., O'Leary, M.J., McCulloch, M. 2007. Global sea-level fluctations during the Last Interglaciation (MIS 5e). Quaternary Science Reviews 26, 2090-2112

Hendey, Q.B., Volman, T.P. 1986. Last interglacial sea-levels and coastal caves in the Cape Province, South Africa. Quaternary Research 25, 189-98

Illenberger, W.K., 1996. The geomorphic evolution of the Wilderness dune cordons, South Africa. Quaternary International, 33, 11–20.

Jacobs, Z., Wintle, A.G. & Duller, G.A.T. 2003. Optical dating of dune sand from Blombos Cave, South Africa: I—multiple grain data. Journal of Human Evolution 44, 599–612

Kaufman, A., Broecker, W.S., Ku, T.L., Thurber, D.L. 1971. The status of U-series methods of mollusk dating. Geochimica et Cosmochimica Acta 35, 1155–1183

Kaufman, D.S. and Manley, W. F., 1998. A new procedure for determining DL amino acid ratios in fossils using reverse phase liquid chromatography. Quaternary Science Reviews 17, 987-1000.

602 Kukla, G.J. 2000. The Last Interglacial. Science 287, 987-988.

603 Lambeck, K., Chappell, J., 2001. Sea-level change through the last glacial cycle. Science 292,

604 679–686.

605 Lambeck, K., Esat, T.M., Potter, E.K. 2002. Links between climate and sea-levels during the

606 past three million years. Nature 419, 199-206

607 Leeder, M.R., 1982. Sedimentology Process and Product. Unwin Hyman: London.

608 Lisiecki, L.E., Raymo, M.E. 2005. A Pliocene-Pleistocene stack of 57 globally distributed

609 benthic $\delta^{18}O$ records. Paleoceanography VOL. 20, PA1003, doi:10.1029/2004PA001071

610 Malan, J.A. 1990. The stratigraphy and sedimentology of the Bredasdorp Group, southern Cape

611 Province. Unpublished MSc Thesis, University of Cape Town.

612 Marean, C.W. Bar-Matthews, M., Bernatchez, J., Fisher., E., Goldberg., P., Herries, A.I.R.,

613 Jacobs., Z., Jerardino, A., Karkanas, P., Minichillo, T., Nilssen, P.J., Thompson, E.,

614 Watts, I., Williams, H.M. 2007. Early Human use of marine resources and pigment in

615 South Africa during the Middle Pleistocene. Nature 449, 905-909.

616 Marker, M.E. 1987. A note on marine benches of the southern Cape. South African Journal of

617 Geology 90, 120-124

618 Marker, M.E., Holmes, P.J. 2005. Landscape evolution and landscape sensitivity: the case of the

619 southern Cape. South African Journal of Science 101, 53-60.

620 Marsh, R.E., Prestwich, W.V., Rink W.J, Brennan, B. J. 2003. Monte Carlo determinations of the

621 beta dose rate to tooth enamel. Radiation Measurements 35, 609-616

622 Martin, A.R.H. 1962. Evidence relating to the Quaternary history of the Wilderness lakes.

623 Transactions of the Geological Society of South Africa 65, 19-45.

624

625 Martinson, D.G., Pisias, N.G., Hays, J.D., Imbrie, J, Moore, T.C., Shackleton, N.J. 1987. Age
626 dating and the Orbital Theory of the Ice Ages - Development of a High-Resolution 0 to
627 300,000-year chronostratigraphy. Quaternary Research 27, 1-29.
628 Massari, F., and Parea, G. C. 1988. Progradational gravel beach sequences in a moderate- to
629 high-energy, microtidal marine environment. Sedimentology 35, 881-913.
630 Maud, R.R. 1968. Quaternary Geomorphology and soil formation in coastal Natal. Zeitschrift für
631 Geomorphologie N.F. Suppl. 7, 135-165.
632 McLaren S.J. Rowe P.J. 1996. The reliability of uranium-series mollusc dates from the Western
633 Mediterranean basin. Quaternary Science Reviews 15, 709–717.
634 Mejdahl, V. 1979 Thermoluminescence dating - Beta-dose attenuation in quartz grains.
635 Archaeometry 21, 61-72
636 Muhs, D.R., 2002. Evidence for the timing and duration of the Last Interglacial period from
637 high-precision uranium-series ages of corals on tectonically stable coastlines. Quaternary
638 Research 58, 36-40.
639 Muhs, D.R., Wehmiller, J.F., Simmons, K.R., York, L.L. 2004. Quaternary sea-level history of
640 the United States. In Gillespie, A.R., Porter, S.C., Atwater, B.F. (eds); *The Quaternary*
641 *Period in the United States: Developments in Quaternary Science* 1, 147-183
642 Munsell Color. 1994. Munsell Soil Color Charts. Macbeth: New Windsor.
643 Murray, A.S., Wintle A.G., 2000. Luminescence dating of quartz using an improved single-
644 aliquot regenerative-dose protocol. Radiation Measurements 32, 57-73.
645 Murray, A.S., Wintle, A.G., 2003. The single aliquot regenerative dose protocol: potential for
646 improvements in reliability. Radiation Measurements 37, 377-381.

647 Murray-Wallace, C. V. 2000. Quaternary coastal aminostratigraphy: Australian data in global
648 context. In G.A. Goodfriend (Eds), Perspectives in Amino Acid and Protein
649 Geochemistry. Oxford University Press Oxford, UK, pp 279-300
650 Murray-Wallace, C.V. 2002. Pleistocene coastal stratigraphy, sea-level highstands and
651 neotectonism of the southern Australian passive continental margin - a review. Journal of
652 Quaternary Science 17, 469-489.
653 Murray-Wallace, C.V. Belperio, A.P. 1991. The last interglacial shoreline in Australia: a review.
654 Quaternary Science Reviews 10, 441-461.
655 Non-affiliated Soil Analysis Working Committee. 1990. Handbook of Standard Soil Testing
656 Methods for Advisory Purposes. Soil Science Society: Pretoria.
657 O'Leary, M.J., Hearty, P.J., McCulloch, M.T. 2008. Geomorphic evidence of major sea-level
658 fluctuations during marine isotope substage-5e, Cape Cuvier, Western Australia.
659 Geomorphology 102, 595-602
660 Overpeck**,** J.T., Otto-Bliesner, B.L., Miller, G.H. Muhs, D.R. Alley, R.B. Kiehl, J.T. 2006.
661 Paleoclimatic Evidence for Future Ice-Sheet Instability and Rapid Sea-Level Rise.
662 Science 311, 1747-1750
663 Prescott, J.R., Hutton, J.T., 1994. Cosmic ray contributions to dose rates for luminescence and
664 ESR dating: large depths and long-term variations. Radiation Measurements 23, 497-500.
665 Ramsay, P.J., Cooper, J.A.G. 2002. Late Quaternary sea-level change in South Africa.
666 Quaternary Research 57, 82-90.
667 Reddering, J.S.V. 1983. An inlet sequence produced by the migration of a small microtidal inlet
668 against longshore drift: the Keurbooms Inlet, South Africa. Sedimentology 30, 201-218

669 Roberts, D., Berger, L.R. 1997. Last interglacial human footprints from South Africa. South
670 African Journal of Science 93, 349-350
671 Roberts, D.L., Bateman, M.D., Murray-Wallace, C.V., Carr, A.S., Holmes, P.J. 2008. Last
672 Interglacial fossil elephant trackways in coastal eolianites, Still Bay, South Africa.
673 Palaeogeography Palaeoclimatology Palaeoecology 257, 261-279.
674 Roberts, D.L., Bateman, M.D., Murray-Wallace, C.V., Carr, A.S., Holmes, P.J. 2009. West
675 Coast Dune Plumes: climate driven contrasts in dunefield morphogenesis along the
676 western and southern South African Coasts. Palaeogeography Palaeoclimatology
677 Palaeoecology 271, 34-48
678 Short, A. D. 1984. Beach and nearshore facies: Southeast Australia. Marine Geology 60, 261-
679 282.
680 Siesser, W.G., Rogers, J. 1970. An investigation of the suitability of four methods used in routine
681 carbonate analysis of marine sediments. Deep Sea Research 18, 135-139.
682 Speed, R.C., Cheng, H. 2004. Evolution of marine terraces and sea level in the last interglacial,
683 Cave Hill, Barbados. Geological Society of America Bulletin 116, 219-232.
684 Stirling, C.H., Esat, T.M., McCulloch, M.T., Lambeck, K., 1995. High-precision U-series dating
685 of corals from Western Australia and implications for the timing and duration of the last
686 interglacial: Earth and Planetary Science Letters 135, 115–130.
687 Stirling, C.H., Esat, T.M., Lambeck, K., McCulloch, M.T. 1998. Timing and duration of the Last
688 Interglacial: evidence for a restricted interval of widespread coral reef growth. Earth and
689 Planetary Science Letters 160, 745-762
690 Tankard, A.J. 1976. The Pleistocene history and coastal morphology of the Ysterfontein-Elands
691 Bay area, Cape Province. Annals of the South African Museum 69, 73-119.

692 Tomazelli. L.J., Dillenburg, S.R. 2007. Sedimentary facies and stratigraphy of a last interglacial
693 coastal barrier in south Brazil. Marine Geology 244, 33-45
694 Tucker M. (ed). 1988. Techniques in Sedimentology. Blackwell: Oxford.
695 U.S. Department of Commerce, National Oceanic and Atmospheric Administration, National
696 Geophysical Data Center, 2006. 2-minute Gridded Global Relief Data (ETOPO2v2)
697 http://www.ngdc.noaa.gov/mgg/fliers/06mgg01.html
698 Waelbroeck, C., Labeyrie, L., Michel, E., Duplessy, J.C., McManus, J.F., Lambeck, K., Balbon,
699 E., Labracherie, M. 2002. Sea-level and deep water temperature changes derived from
700 benthonic foraminifera isotopic records: Quaternary Science Reviews 21, 295–305
701 Waelbroeck, C., Frank, N., Jouzel, J., Parrenin, F. Masson-Delmotte, V. Genty, D. 2008.
702 Transferring radiometric dating of the last interglacial sea level highstand to marine and
703 ice core records. Earth and Planetary Science Letters 265, 183-194
704 Woodroffe, C.D., Murray-Wallace, C.V., Bryant, E.A., Brooke, B., Heijnis, H., Price, D.M.
705 1995. Late Quaternary sea-level highstands in the Tasman Sea - evidence from Lord-
706 Howe Island. Marine Geology 125, 61-72
707 Woodroffe, S.A., Horton, B.P. 2005. Holocene sea-level changes in the Indo-Pacific. Journal of
708 Asian Earth Sciences 25, 29-43.
709 Young, R.W., Bryant, E.A., Price, D. 1993. Last Interglacial sea levels on the South Coast of
710 New South Wales. Australian Geographer 24, 72–75.